POLISH MARITIME RESEARCH 3 (115) 2022 Vol. 29; pp. 47-60
10.2478/pomr-2022-0025

AN IMPROVED DYNAMIC SURFACE SLIDING MODE METHOD FOR AUTONOMOUS COOPERATIVE FORMATION CONTROL OF UNDERACTUATED USVS WITH COMPLEX MARINE ENVIRONMENT DISTURBANCES

Zaopeng Dong[1, 2, 3]
Shijie Qi[1, 3]
Min Yu[1, 3*]
Zhengqi Zhang[1, 3]
Haisheng Zhang[1, 3]
Jiakang Li[1, 3]
Yang Liu[1, 3]

[1] Key Laboratory of High Performance Ship Technology (Wuhan University of Technology), Ministry of Education, Wuhan University of Technology, Wuhan, China
[2] Science and Technology on Underwater Vehicle Technology Laboratory, Harbin Engineering University, Harbin, China
[3] School of Naval Architecture, Ocean and Energy Power Engineering, Wuhan University of Technology, Wuhan, China

* Corresponding author: *yumin@whut.edu.cn* (Min Yu)

ABSTRACT

In this paper, a novel dynamic surface sliding mode control (DSSMC) method, combined with a lateral velocity tracking differentiator (LVTD), is proposed for the cooperative formation control of underactuated unmanned surface vehicles (USVs) exposed to complex marine environment disturbances. Firstly, in view of the kinematic and dynamic models of USVs and the design idea of a virtual control law in a backstepping approach, the trajectory tracking control problem of USVs' cooperative formation is transformed into a stabilisation problem of the virtual control law of longitudinal and lateral velocities. Then, aiming at the problem of differential explosion caused by repeated derivation in the process of backstepping design, the first-order low-pass filter about the virtual longitudinal velocity and intermediate state quantity of position is constructed to replace differential calculations during the design of the control law, respectively. In order to reduce the steady-state error when stabilising the virtual lateral velocity control law, the integral term is introduced into the design of the sliding mode surface with a lateral velocity error, and then the second-order sliding mode surface with an integral is structured. In addition, due to the problem of controller oscillation and the role of the tracking differentiator (TD) in active disturbance rejection control (ADRC), the LVTD is designed to smooth the state quantity of lateral velocity. Subsequently, based on the dynamic model of USV under complex marine environment disturbances, the nonlinear disturbance observer is designed to observe the disturbances and compensate the control law. Finally, the whole cooperative formation system is proved to be uniformly and ultimately bounded, according to the Lyapunov stability theory, and the stability and validity of the method is also verified by the simulation results.

Keywords: underactuated USV, dynamic surface sliding mode control, lateral velocity tracking differentiator, nonlinear disturbance observer

INTRODUCTION

In recent years, marine science and technology has been developed, in order to explore the ocean [1, 2]. Meanwhile, because of the development and advancement of technologies in robotics and autonomous systems (RAS) [3], research on unmanned surface vessels (USVs) motion control has gradually become a hot topic [4-7], with USVs also playing an increasingly essential role in various fields, e.g. military defence, scientific research, environmental monitoring and so on [8-10]. However, with marine operations becoming more and more complex and diversified, a single USV cannot complete a mission well, owing to limitations such as limited information perception [11-13]. Consequently, cooperative formation control of USVs has aroused great attention in recent years, on account of the high fault tolerance, strong adaptability and robustness and cooperative formation control of underactuated USVs [14, 15].

The commonly used formation control strategies include the leader-follower method, behaviour-based method, virtual structure method and graph theory method. The leader-follower method is widely applied because it is simple and easy to use. The leader-follower method was combined with multi-layer neural network and adaptive robust techniques in [16], and the output feedback formation control problem for USVs with limited torque input was solved. In [17], a formation controller for a group of underactuated USVs was designed as an adaptive feedback control problem for a line of sight (LOS) based configuration of a leader and a follower. Design of the controller took time-varying constraints on the LOS and bearing angle into consideration and used asymmetric barrier Lyapunov functions. Similarly, the leader-follower method, LOS strategy and neural networks were used in [18], for designing the formation controller of a waterjet USV, exposed to unmodelled dynamics, environmental disturbances, input saturation, and output constraints. A USV formation approach, based on a distributed deep reinforcement learning algorithm, was proposed in [19], which made formations to arbitrarily increase the number of USVs or change formation forms. In [20], model predictive control was used to deal with vessel train formation (VTF) problems including cooperative collision avoidance and grouping of vessels; a single-layer serial iterative architecture was adopted in distributed formulation, for reducing communication requirements and improving robustness against failures. Both the unmeasurable velocity and external disturbances were estimated by a new finite-time extended state observer in [21] and derivatives of external disturbances for time need not be zero. Then a distributed finite-time formation controller was designed based on the above estimator. In [22] a sliding mode control approach and adaptive algorithms were applied to address the problem of the finite-time distributed formation control for USVs with model uncertainties, input saturation constraints and ocean disturbances. The unavailable system dynamics were approached by radial basis function neural networks (RBFNNs) and the minimum learning parameter (MLP) algorithm was adopted for simplifying the calculations. Utilising the prescribed performance control method, neural network approximation, disturbance observers, dynamic surface control technique, and Lyapunov synthesis, a formation controller was designed to make USVs exposed to model uncertainties and time-varying external disturbances follow the desired trajectory in [23]. In [24], because the industrial applications of multi-marine vehicles systems needed to provide a realistic setup, a new collision-free distributed formation control method for underactuated USVs networks was proposed, which included a distributed coordination layer and a local fixed-time neural network control layer. An original fault tolerant leader-follower formation control project for a batch of underactuated USVs, which possessed partially known control input gain functions, was proposed in [25]. Simultaneously, the LOS range and angle tracking errors were demanded for constraint. In [26], in order to handle the leader-follower formation problem for several underactuated USVs when model uncertainties and environmental disturbances existed, a novel formation control scheme with robustness and adaptability, containing the MLP algorithm and the disturbance observer (DOB), was presented. An adaptive observer combined with neural networks was used to evaluate the velocity information of USVs and the unknown nonlinearities were estimated by neural networks in [27], solving the problem of connectivity preservation and collision avoidance among networked uncertain underactuated USVs with different communication ranges. In [28], on account of the problem for optimal trajectory tracking of a maritime autonomous surface ship (MASS), which was affected by inherent dynamic uncertainties and the time-varying external disturbances resulting from wind, waves and currents, the modified optimal adaptive super-twisting sliding mode control (OAST-SMC) algorithm was designed as a robust optimal adaptive strategy. Integrating sliding mode control and fuzzy control, a novel control scheme was presented in [29] and, in order to structure heterogeneous multi-agent unmanned formation systems mission requirements, an artificial potential field method and leader-follower method were used to solve the problem of unmanned aerial vehicle and unmanned surface vehicle (UAV-USV) formation motion control. In [30], because of a limited communication range, a distributed event-triggered tracking approach with robustness was proposed and the network connectivity and tracking performance of the formation system was guaranteed. In the meantime, in order to maintain connectivity of the formation system and avoid collisions with each other, a formation tracking controller of uncertain underactuated USVs (based on the leader-follower method) was designed by reducing connectivity-maintaining and collision-avoiding performance functions and constructing an obstacle avoidance strategy in the connectivity between the leader and followers in [31]. The paper by [32] presents an active disturbance rejection control (ADRC) and uncertain parameters, non-linearities, and external disturbances were all considered as parts of the disturbance, which is estimated in real-time by the Extended State Observer (ESO). Then the position and path-following control of a fully actuated

autonomous underwater vehicle (AUV) was solved. An efficient controller was designed through a backstepping technique for the case of full-state feedback in the presence of unknown external disturbances, and the dynamic positioning problem for autonomous surface ships was solved in [33]. In the meantime, the obtained control commands were distributed to each actuator of the overactuated vessel via unconstrained control allocation.

Summarising the above literature on cooperative formation control of USVs, the backstepping approach was adopted in most of the research and a lot of quantities needed to be derived during the design of a controller. However, a phenomenon known as 'differential explosion' can emerge after multiple derivatives, which makes the design process of the controller become complex and is unfavourable to engineering practice. Therefore, the novel dynamic surface sliding mode control (DSSMC) method in this paper is presented to solve this problem. The contributions of this paper are as follows: (i) After comprehensive consideration of the core idea for dynamic surface control, an improved sliding mode control method is applied to design a formation controller; (ii) Referring to the core idea of the backstepping approach, longitudinal velocity and lateral velocity virtual control laws are designed for the convenience of subsequent controller design; (iii) The integral term of lateral velocity error is introduced, to construct the second-order sliding surface with an integral for reducing steady-state error when stabilising the virtual lateral velocity; (iv) Considering the role of TD in ADRC, the lateral velocity tracking differentiator (LVTD) is designed to smooth the lateral velocity and avoid control law oscillation; (v) In order to approach marine environment disturbances and simplify the controller, the nonlinear disturbance observer, linked with a dynamic model of USV, is adopted to observe and compensate disturbances.

This paper is organised as follows. USV motion models and a description of a cooperative formation trajectory tracking control problem are arranged in Section 2. The control law is designed and the stability of the control law is proved in Section 3. In Section 4, simulation experiments are carried out, which verify the accuracy and effectiveness of the controller. Ultimately, some conclusions are formulated in Section 5.

PROBLEM FORMULATION

In order to design a USV formation controller, mathematical models of USV motion are formulated, which include kinematic and dynamic models. A problem with a USV formation model will be described in this section.

MATHEMATICAL MODELS OF USV

Supposing there are $N+1$ members in the system of USV formation, one is leader USV and the other N is a follower USV. According to [34], the kinematic models of USVs can be expressed as:

$$\boldsymbol{\eta}_j = \boldsymbol{R}(\psi_j)\boldsymbol{v}_j \tag{1}$$

Each USV is numbered by the subscript j $(j = k+1, k = 0 \cdots N)$, and where $\boldsymbol{\eta}_j = [x_j, y_j, \psi_j]^T$ and $\boldsymbol{v}_j = [u_j, v_j, r_j]^T$. (x_j, y_j) denotes the position coordinates of USV in the earth-fixed inertial frame; ψ_j is the heading angle; (u_j, v_j, r_j) represent the velocity vectors for the jth USV in the surge, sway and yaw directions in the body-fixed frame, respectively. $\boldsymbol{R}(\psi_j)$ is the rotation matrix of yaw, as follows:

$$\boldsymbol{R}(\psi_j) = \begin{bmatrix} \cos\psi_j & -\sin\psi_j & 0 \\ \sin\psi_j & \cos\psi_j & 0 \\ 0 & 0 & 1 \end{bmatrix}$$

The nonlinear dynamic model of USV with external environmental disturbances is described as:

$$\boldsymbol{M}_j\dot{\boldsymbol{v}}_j + \boldsymbol{C}(v_j)\boldsymbol{v}_j + \boldsymbol{D}(v_j)\boldsymbol{v}_j = \boldsymbol{\tau}_j + \boldsymbol{d}_j \tag{2}$$

where $\boldsymbol{M}_j$ is the system inertia matrix (including added mass) of the jth USV; $\boldsymbol{C}_j$ represents a Coriolis-centripetal matrix (including added mass); $\boldsymbol{D}_j$ is the hydrodynamic damping coefficients matrix of the jth USV; and $\boldsymbol{d}_j$ is the vector of environmental disturbance forces and moment acting on the jth USV:

$$\boldsymbol{M}_j = \begin{bmatrix} m_{1j} & 0 & 0 \\ 0 & m_{2j} & 0 \\ 0 & 0 & m_{3j} \end{bmatrix}, \boldsymbol{D}(v_j) = \begin{bmatrix} d_{1j} & 0 & 0 \\ 0 & d_{2j} & 0 \\ 0 & 0 & d_{3j} \end{bmatrix} \quad \boldsymbol{C}(v_j) = \begin{bmatrix} 0 & 0 & -m_{2j}v_j \\ 0 & 0 & m_{1j}u_j \\ m_{2j}v_j & -m_{1j}u_j & 0 \end{bmatrix}$$

$$\boldsymbol{d}_j = [d_{uj}, d_{vj}, d_{rj}]^T$$

Equation (1) and (2) are unfolded and combined, and models of USV with three degrees of mathematical freedom can be obtained, as:

$$\begin{cases} \dot{x}_j = u_j\cos\psi_j - v_j\sin\psi_j \\ \dot{y}_j = u_j\sin\psi_j + v_j\cos\psi_j \\ \dot{\psi}_j = r_j \\ \dot{u}_j = \dfrac{m_{2j}}{m_{1j}}v_jr_j - \dfrac{d_{1j}}{m_{1j}}u_j + \dfrac{1}{m_{1j}}\tau_{uj} + \dfrac{1}{m_{1j}}d_{uj} \\ \dot{v}_j = -\dfrac{m_{1j}}{m_{2j}}u_jr_j - \dfrac{d_{2j}}{m_{2j}}v_j + \dfrac{1}{m_{2j}}d_{vj} \\ \dot{r}_j = \dfrac{m_{1j} - m_{2j}}{m_{3j}}u_jv_j - \dfrac{d_{3j}}{m_{3j}}r_j + \dfrac{1}{m_{3j}}\tau_{rj} + \dfrac{1}{m_{3j}}d_{rj} \end{cases} \tag{3}$$

DESCRIPTION OF COOPERATIVE FORMATION CONTROL OF USV

In order to simply and conveniently design a cooperative formation controller of a USV, the leader-follower method is adopted in this paper. The core of the leader-follower method means that one of this group is designated as the leader for all of the formation system and the remainder members are known as followers; moreover, the leader of the whole formation is tracked by followers in a certain relative position and attitude. The diagram of the cooperative formation model of USVs is established in the earth-fixed frame, as follows:

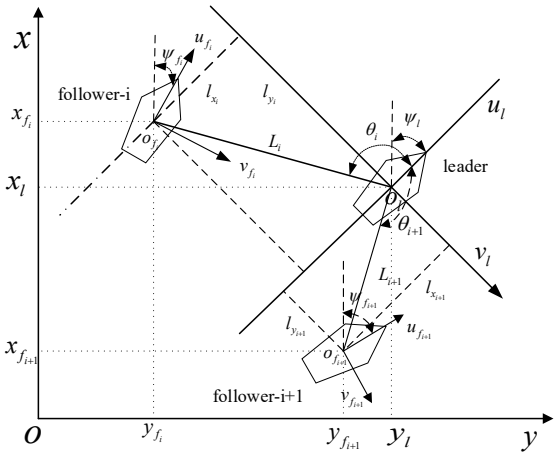

Fig. 1. Diagrammatic sketch of USVs formation

where (x_l, y_l, ψ_l) and $(x_{f_i}, y_{f_i}, \psi_{f_i})$ denote the position coordinates and heading angle of the leader USV and the ith $(i = 1, 2\cdots, N-1)$ follower in the earth-fixed frame, respectively; (u_l, v_l) and (u_{f_i}, v_{f_i}) represent the velocity vectors for the leader USV and the ith $(i = 1, 2\cdots, N-1)$ follower USV in the surge and sway directions in the body-fixed frame; (L_i, θ_i) ($\theta_i \in [-\pi, \pi]$, positive clockwise) are the distance and angle between the leader USV and the ith follower USV; (l_{x_i}, l_{y_i}) indicate the relative longitudinal and lateral distance between the leader USV and the ith follower USV in the leader-fixed frame.

According to the principle of the leader-follower method, when the USV formation is formulated, both L_i and θ_i are fixed values in the earth-fixed frame; meanwhile l_{x_i} and l_{y_i} are fixed values too. From Fig. 1, the desired relative longitudinal distance $l_{x_i d}$ and lateral distance $l_{y_i d}$ between the leader USV and the ith follower USV are as below:

$$\begin{cases} l_{x_i d} = (x_{f_i d} - x_l)\cos\psi_l + (y_{f_i d} - y_l)\sin\psi_l \\ l_{y_i d} = -(x_{f_i d} - x_l)\sin\psi_l + (y_{f_i d} - y_l)\cos\psi_l \end{cases} \tag{4}$$

Equation (4) can also be written as:

$$\begin{bmatrix} l_{x_i d} \\ l_{y_i d} \end{bmatrix} = \begin{bmatrix} \cos\psi_l & \sin\psi_l \\ -\sin\psi_l & \cos\psi_l \end{bmatrix} \begin{bmatrix} x_{f_i d} - x_l \\ y_{f_i d} - y_l \end{bmatrix} \tag{5}$$

The $l_{x_i d}$ and $l_{y_i d}$ are rotated from the body-fixed frame to the earth-fixed frame and the desired trajectory $(x_{f_i d}, y_{f_i d})$ of the ith follower USV in the earth-fixed frame can be obtained as:

$$\begin{cases} y_{f_i d} = y_l + l_{y_i d}\cos\psi_{ld} + l_{x_i d}\sin\psi_l \\ x_{f_i d} = x_l + l_{x_i d}\cos\psi_{ld} - l_{y_i d}\sin\psi_l \end{cases} \tag{6}$$

Therefore, the problem of the cooperative formation control of a group of USVs can be transformed into the trajectory tracking control of each USV in the group. Furthermore, the purpose of formation control can be changed as:

$$\begin{cases} \lim\limits_{t\to\infty} \left\| x_{f_i} - x_{f_i d} \right\| = 0 \\ \lim\limits_{t\to\infty} \left\| y_{f_i} - y_{f_i d} \right\| = 0 \end{cases} \tag{7}$$

CONTROLLER DESIGN

NONLINEAR DISTURBANCE OBSERVER

During navigation, USV formation systems are subject to unknown marine disturbances. In order to observe and compensate for disturbances, a nonlinear disturbance observer is designed [35] as follows:

$$\begin{cases} \hat{d} = z + p(\theta, \dot{\theta}) \\ \dot{z} = -L(\theta, \dot{\theta})z + L(\theta, \dot{\theta})[G(\theta, \dot{\theta}) - T - p(\theta, \dot{\theta})] \end{cases} \tag{8}$$

Mathematical models of USV are combined with Eq. (8), as:

$$\begin{cases} \hat{\boldsymbol{d}}_j = \boldsymbol{Z}_j + \boldsymbol{L}_j \boldsymbol{M}_j \boldsymbol{v}_j \\ \dot{\boldsymbol{Z}}_j = -\boldsymbol{L}_j \hat{\boldsymbol{d}}_j - \boldsymbol{L}_j[-\boldsymbol{C}(v_j)\boldsymbol{v}_j - \boldsymbol{D}(v_j)\boldsymbol{v}_j + \boldsymbol{\tau}_j] \end{cases} \tag{9}$$

where $\boldsymbol{Z}_j = [Z_{ju}, Z_{jv}, Z_{jr}]^T$ is structural quantity; $\boldsymbol{L}_j = [L_{ju}, L_{jv}, L_{jr}]^T$ are the bandwidth parameters of the observer; and $\hat{\boldsymbol{d}}_j = [\hat{d}_{uj}, d_{vj}, d_{rj}]^T$ are observations of ocean disturbances.

Simultaneously, it must be considered that actual marine disturbances fluctuate slowly. In the following section, $\dot{\boldsymbol{d}}_j$ is assumed to be bounded and expressed as $\left|\dot{\boldsymbol{d}}_j\right| \le \sigma$, $(\sigma \ge 0)$. The error between observation and real disturbances is defined as:

$$\tilde{\boldsymbol{d}}_j = \hat{\boldsymbol{d}}_j - \boldsymbol{d}_j = [\hat{d}_{uj} - d_{uj}, d_{vj} - d_{vj}, d_{rj} - d_{rj}]^T \tag{10}$$

A derivation and simplification of Eq. (9) is:

$$\begin{aligned}\dot{\tilde{\boldsymbol{d}}}_j &= \dot{\hat{\boldsymbol{d}}}_j - \dot{\boldsymbol{d}}_j \\ &= \dot{\boldsymbol{Z}}_i + \boldsymbol{L}_j\boldsymbol{M}_j\dot{\boldsymbol{v}}_j - \dot{\boldsymbol{d}}_j \\ &= -\boldsymbol{L}_j\hat{\boldsymbol{d}}_j - \boldsymbol{L}_j[-\boldsymbol{C}(v_j)\boldsymbol{v}_j - \boldsymbol{D}(v_j)\boldsymbol{v}_j + \boldsymbol{\tau}_j] + \boldsymbol{L}_j\boldsymbol{M}_j\dot{\boldsymbol{v}}_j - \dot{\boldsymbol{d}}_j \\ &= -\boldsymbol{L}_j\hat{\boldsymbol{d}}_j - \boldsymbol{L}_j[-\boldsymbol{C}(v_j)\boldsymbol{v}_j - \boldsymbol{D}(v_j)\boldsymbol{v}_j + \boldsymbol{\tau}_j - \boldsymbol{M}_j\dot{\boldsymbol{v}}_j] - \dot{\boldsymbol{d}}_j \\ &= -\boldsymbol{L}_j\hat{\boldsymbol{d}}_j + \boldsymbol{L}_j\boldsymbol{d}_j - \dot{\boldsymbol{d}}_j = -\boldsymbol{L}_j\tilde{\boldsymbol{d}}_j - \dot{\boldsymbol{d}}_j\end{aligned} \tag{11}$$

Based on the above assumption, the first order differential inequality on observation error can be gained as:

$$\dot{\tilde{\boldsymbol{d}}}_j + \boldsymbol{L}_j\tilde{\boldsymbol{d}}_j \le \left|\dot{\boldsymbol{d}}_j\right| = \sigma \tag{12}$$

Equation (12) is solved as:

$$0 \le \tilde{\boldsymbol{d}}_j(t) \le \frac{\sigma}{\boldsymbol{L}_j} + [\tilde{\boldsymbol{d}}_j(0) - \frac{\sigma}{\boldsymbol{L}_j}]e^{-\boldsymbol{L}_j t} \tag{13}$$

According to Eq. (13), by selecting appropriate bandwidth parameters, the observation error can finally be stabilised.

DESIGN CONTROLLER OF FOLLOWER

The controller is designed in this part. Firstly, the virtual velocity control law can be obtained based on positive definite position error. Then, the surge force and yaw moment can be designed by stabilising the virtual velocity control law.

DESIGN VIRTUAL VELOCITY CONTROL LAW

The position error state quantity of the ith follower is defined as:

$$\begin{bmatrix} x_{f_ie} \\ y_{f_ie} \end{bmatrix} = \begin{bmatrix} x_{f_i} - x_{f_id} \\ y_{f_i} - y_{f_id} \end{bmatrix} \tag{14}$$

The derivation of Eq. (14) is as:

$$\begin{bmatrix} \dot{x}_{f_ie} \\ \dot{y}_{f_ie} \end{bmatrix} = \begin{bmatrix} \dot{x}_{f_i} - \dot{x}_{f_id} \\ \dot{y}_{f_i} - \dot{y}_{f_id} \end{bmatrix} = \begin{bmatrix} \cos(\psi_{f_i}) & -\sin(\psi_{f_i}) \\ \sin(\psi_{f_i}) & \cos(\psi_{f_i}) \end{bmatrix} \begin{bmatrix} u_{f_i} \\ v_{f_i} \end{bmatrix} - \begin{bmatrix} \dot{x}_{f_id} \\ \dot{y}_{f_id} \end{bmatrix} \tag{15}$$

The Lyapunov function is constructed as follows:

$$V_i = \frac{1}{2}x_{f_ie}{}^2 + \frac{1}{2}y_{f_ie}{}^2 \tag{16}$$

Derivation and simplification of Eq. (16) is as below:

$$\begin{aligned}\dot{V}_i &= x_{f_ie}\dot{x}_{f_ie} + y_{f_ie}\dot{y}_{f_ie} \\ &= x_{f_ie}(u_{f_i}\cos\psi_{f_i} - v_{f_i}\sin\psi_{f_i} - \dot{x}_{f_id}) + y_{f_ie}(u_{f_i}\sin\psi_{f_i} + v_{f_i}\cos\psi_{f_i} - \dot{y}_{f_id})\end{aligned} \tag{17}$$

Through the analysis of Eq. (17), virtual velocity control law α_{f_iu} and α_{f_iv} in the surge and sway directions, are devised as:

$$\begin{bmatrix} \alpha_{f_iu} \\ \alpha_{f_iv} \end{bmatrix} = \begin{bmatrix} \cos(\psi_{f_i}) & \sin(\psi_{f_i}) \\ -\sin(\psi_{f_i}) & \cos(\psi_{f_i}) \end{bmatrix} \begin{bmatrix} \dot{x}_{f_id} - k_{1_i}x_{f_ie} / \sqrt{x^2_{f_ie} + y^2_{f_ie} + C_{f_i}} \\ \dot{y}_{f_id} - k_{2_i}y_{f_ie} / \sqrt{x^2_{f_ie} + y^2_{f_ie} + C_{f_i}} \end{bmatrix} \tag{18}$$

where k_{1_i}、k_{2_i}、C_{f_i} are all positive numbers; and $\sqrt{x^2_{f_ie} + y^2_{f_ie} + C_{f_i}}$ is denoted by w_{f_i}.

DESIGN THE SURGE FORCE CONTROL LAW

The velocity error of the ith follower USV in the surge and sway directions are defined as $u_{f_ie} = u_{f_i} - \alpha_{f_iu}$, $v_{f_ie} = v_{f_i} - \alpha_{f_iv}$, respectively.

In order to reduce steady-state error, an integral term of u_{f_ie} is added to the sliding surface, when u_{f_ie} is stabilised and the surge force of the ith follower is designed. The integral first-order sliding surface is constructed as follows:

$$s_{1_i} = u_{f_ie} + \lambda_{1_i}\int_0^t u_{f_ie}(\tau)d\tau,\ (\lambda_{1_i} > 0) \tag{19}$$

substituting Eq. (3) into derivation of Eq. (19) as:

$$\begin{aligned}\dot{s}_{1_i} &= \dot{u}_{f_ie} + \lambda_{1_i}u_{f_ie} = \dot{u}_{f_i} - \dot{\alpha}_{f_iu} + \lambda_{1_i}u_{f_ie} \\ &= \frac{m_{2j}}{m_{1j}}v_{f_i}r_{f_i} - \frac{d_{1j}}{m_{1j}}u_{f_i} + \frac{1}{m_{1j}}\tau_{f_iu} + \frac{1}{m_{1j}}\tilde{d}_{uj} - \dot{\alpha}_{f_iu} + \lambda_{1_i}u_{f_ie}\end{aligned} \tag{20}$$

In order to avoid differential explosion, the first order low pass filter is applied. The new state quantity X_{f_iu} is introduced and defined as the output of the first order low pass filter. $\dot{\alpha}_{f_iu}$ is replaced with a derivation of it. The mathematical expression is as follows [36]:

$$\begin{cases} T_{1_i}\dot{X}_{f_iu} + X_{f_iu} = \alpha_{f_iu} \\ X_{f_iu}(0) = \alpha_{f_iu}(0),\ (T_{1_i} > 0) \end{cases} \tag{21}$$

Equation (20) is obtained:

$$\dot{X}_{f_iu} = (\alpha_{f_iu} - X_{f_iu})/T_{1_i} \tag{22}$$

In order to avoid the buffeting problem caused by designing the control law with a symbolic function, the reaching law of sliding mode control with hyperbolic tangent function is adopted in this paper.

$$\dot{s}_{1_i} = -\varepsilon_{1_i}\tanh(s_{1_i}) - \eta_{1_i}s_{1_i},\ (\varepsilon_{1_i} > 0, \eta_{1_i} > 0) \tag{23}$$

Substituting Eq. (23) into Eq. (20), the surge force of the ith follower USV can be obtained as:

$$\tau_{f_iu} = m_{1j}[-\frac{1}{m_{1j}}\tilde{d}_{uj} - \frac{m_{2j}}{m_{1j}}v_{f_i}r_{f_i} + \frac{d_{1j}}{m_{1j}}u_{f_i} + \dot{X}_{f_iu} - \lambda_{1_i}u_{f_ie} - \varepsilon_{1_i}\tanh(s_{1_i}) - \eta_{1_i}s_{1_i}] \tag{24}$$

DESIGN THE YAW MOMENT CONTROL LAW

Due to the underactuated characteristics of the research object and the lack of input in the sway direction, the second-order sliding surface of $v_{f_i e}$ is designed to make the yaw moment $\tau_{f_i r}$ appear. At the same time, in order to reduce steady-state error when tracking a straight trajectory, the integral term of $v_{f_i e}$ is introduced. The design of sliding surface is as follows:

$$s_{2_i} = \dot{v}_{f_i e} + \lambda_{2_i} v_{f_i e} + \lambda_{3_i} \int_0^t v_{f_i e} dt, \ (\lambda_{2_i} > 0, \lambda_{3_i} > 0) \tag{25}$$

Derivations of Eq. (25) are:

$$\dot{s}_{2_i} = \ddot{v}_{f_i e} + \lambda_{2_i} \dot{v}_{f_i e} + \lambda_{3_i} v_{f_i e} = \ddot{v}_{f_i} - \ddot{\alpha}_{f_i v} + \lambda_{2_i} \dot{v}_{f_i e} + \lambda_{3_i} v_{f_i e} \tag{26}$$

For simplifying Eq. (26), derivations of Eq. (18) are needed as:

$$\begin{aligned} \dot{\alpha}_{f_i v} = & -r_{f_i} \alpha_{f_i u} - [\ddot{x}_{f_i d} - k_{1_i} (w_{f_i}^{-1} - w_{f_i}^{-3} x_{f_i e}^2) \dot{x}_{f_i e} + k_{1_i} w_{f_i}^{-3} x_{f_i e} y_{f_i e} \dot{y}_{f_i e}] \sin(\psi_{f_i}) \\ & + [\ddot{y}_{f_i d} - k_{2_i} (w_{f_i}^{-1} - w_{f_i}^{-3} y_{f_i e}^2) \dot{y}_{f_i e} + k_{2_i} w_{f_i}^{-3} x_{f_i e} y_{f_i e} \dot{x}_{f_i e}] \cos(\psi_{f_i}) \end{aligned} \tag{27}$$

The intermediate quantity is defined as:

$$\begin{aligned} p_{f_i} = & -[\ddot{x}_{f_i d} - k_{1_i} (w_{f_i}^{-1} - w_{f_i}^{-3} x_{f_i e}^2) \dot{x}_{f_i e} + k_{1_i} w_{f_i}^{-3} x_{f_i e} y_{f_i e} \dot{y}_{f_i e}] \sin(\psi_{f_i}) \\ & + [\ddot{y}_{f_i d} - k_{2_i} (w_{f_i}^{-1} - w_{f_i}^{-3} y_{f_i e}^2) \dot{y}_{f_i e} + k_{2_i} w_{f_i}^{-3} x_{f_i e} y_{f_i e} \dot{x}_{f_i e}] \cos(\psi_{f_i}) \end{aligned} \tag{28}$$

Similarly, the first order low pass filter of p_{f_i} is introduced, and p_{f_i} and $\dot{p}_{f_i}$ are replaced with $X_{f_i p}$ and $\dot{X}_{f_i p}$, respectively. The mathematical expression is:

$$\begin{cases} T_{2_i} \dot{X}_{f_i p} + X_{f_i p} = p_{f_i} \\ X_{f_i p}(0) = p_{f_i}(0), \ (T_{2_i} > 0) \end{cases} \tag{29}$$

Equation (29) is obtained:

$$\dot{X}_{f_i p} = (p_{f_i} - X_{f_i p}) / T_{2_i} \tag{30}$$

Then Eq. (27) can be simplified, as:

$$\dot{\alpha}_{f_i v} = X_{f_i p} - r_{f_i} \alpha_{f_i u} \tag{31}$$

Simultaneously, Eq. (26), (30) and (31) are solved as:

$$\dot{s}_{2_i} = \ddot{v}_{f_i} - \dot{X}_{f_i p} + \dot{r}_{f_i} \alpha_{f_i u} + r_{f_i} X_{f_i u} + \lambda_{2_i} \dot{v}_{f_i e} + \lambda_{3_i} v_{f_i e} \tag{32}$$

Similarly, the reaching law of sliding mode control is designed as:

$$\dot{s}_{2_i} = -\varepsilon_{2_i} \tanh(s_{2_i}) - \eta_{2_i} s_{2_i}, \ (\varepsilon_{2_i} > 0, \eta_{2_i} > 0) \tag{33}$$

Eq. (32) and Eq. (33) are simplified, as follows:

$$\dot{r}_{f_i} = (-\ddot{v}_{f_i} + \dot{X}_{f_i p} - r_{f_i} X_{f_i u} - \lambda_{2_i} \dot{v}_{f_i e} - \lambda_{3_i} v_{f_i e} - \varepsilon_{2_i} \tanh(s_{2_i}) - \eta_{2_i} s_{2_i}) / \alpha_{f_i u} \tag{34}$$

Owing to the drastic variation in $\ddot{v}_{f_i}$, the controller is not easily convergent. In order to smooth $\ddot{v}_{f_i}$, LVTD is introduced and applied [35] and the discrete form is as below:

$$\begin{cases} x_{1_i}(k+1) = x_{1_i}(k) + h x_{2_i}(k) \\ x_{2_i}(k+1) = x_{2_i}(k) + h\{-rr_i^2 [x_{1_i}(k) - \dot{v}_{f_i}(k)] - 2rr_i x_{2_i}(k)\} \end{cases} \tag{35}$$

where h is the time step size; rr_i are the control parameters of LVTD; and x_{1_i} and x_{2_i} are all output signals. $\dot{v}_{f_i}$ is replaced with x_{1_i} and x_{2_i} is the differential of x_{1_i} which substitutes for $\ddot{v}_{f_i}$. The yaw moment $\tau_{f_i r}$ of the ith follower can be obtained by simultaneously addressing Eq. (3), (34) and (35) as:

$$\begin{aligned} \tau_{f_i r} &= -(m_{1j} - m_{2j}) u_{f_i} r_{f_i} + d_{3j} r_{f_i} + m_{3j} \dot{r}_{f_i} - \tilde{d}_{rj} \\ &= -\tilde{d}_{rj} - (m_{1j} - m_{2j}) u_{f_i} r_{f_i} + d_{3j} r_{f_i} \\ &\quad + m_{3j} (-x_{2_i} + \dot{X}_{f_i p} - r_{f_i} X_{f_i u} - \lambda_{2_i} \dot{v}_{f_i e} - \lambda_{3_i} v_{f_i e} - \varepsilon_{2_i} \tanh(s_{2_i}) - \eta_{2_i} s_{2_i}) / \alpha_{f_i u} \end{aligned} \tag{36}$$

STABILITY ANALYSIS

In this section, the stability of control law, Eq. (24) and (36), is proved. For the first order low pass filter introduced in the previous section, the filtering error is defined as:

$$\begin{cases} y_{1_i} = X_{f_i u} - \alpha_{f_i u} \\ y_{2_i} = X_{f_i p} - p_{f_i} \end{cases} \tag{37}$$

The derivation of Eq. (37), simultaneously with Eq. (22), (30), and (37), and simplifying, gives:

$$\begin{cases} \dot{y}_{1_i} = -\dfrac{y_{1_i}}{T_{1_i}} + \dfrac{\partial \alpha_{f_i u}}{\partial \dot{x}_{f_i d}} \ddot{x}_{f_i d} + \dfrac{\partial \alpha_{f_i u}}{\partial \dot{y}_{f_i d}} \ddot{y}_{f_i d} + \dfrac{\partial \alpha_{f_i u}}{\partial x_{f_i e}} \dot{x}_{f_i e} + \dfrac{\partial \alpha_{f_i u}}{\partial y_{f_i e}} \dot{y}_{f_i e} + \dfrac{\partial \alpha_{f_i u}}{\partial \psi_{f_i}} \dot{\psi}_{f_i} \\ \dot{y}_{2_i} = -\dfrac{y_{2_i}}{T_{2_i}} + \dfrac{\partial p_{f_i}}{\partial \ddot{x}_{f_i d}} \dddot{x}_{f_i d} + \dfrac{\partial p_{f_i}}{\partial \ddot{y}_{f_i d}} \dddot{y}_{f_i d} + \dfrac{\partial p_{f_i}}{\partial \dot{x}_{f_i e}} \ddot{x}_{f_i e} + \dfrac{\partial p_{f_i}}{\partial \dot{y}_{f_i e}} \ddot{y}_{f_i e} + \dfrac{\partial p_{f_i}}{\partial \psi_{f_i}} \dot{\psi}_{f_i} \end{cases} \tag{38}$$

The new quantities are defined as:

$$\begin{cases} \beta_{1_i} = \dfrac{\partial \alpha_{f_i u}}{\partial \dot{x}_{f_i d}} \ddot{x}_{f_i d} + \dfrac{\partial \alpha_{f_i u}}{\partial \dot{y}_{f_i d}} \ddot{y}_{f_i d} + \dfrac{\partial \alpha_{f_i u}}{\partial x_{f_i e}} \dot{x}_{f_i e} + \dfrac{\partial \alpha_{f_i u}}{\partial y_{f_i e}} \dot{y}_{f_i e} + \dfrac{\partial \alpha_{f_i u}}{\partial \psi_{f_i}} \dot{\psi}_{f_i} \\ \beta_{2_i} = \dfrac{\partial p_{f_i}}{\partial \ddot{x}_{f_i d}} \dddot{x}_{f_i d} + \dfrac{\partial p_{f_i}}{\partial \ddot{y}_{f_i d}} \dddot{y}_{f_i d} + \dfrac{\partial p_{f_i}}{\partial \dot{x}_{f_i e}} \ddot{x}_{f_i e} + \dfrac{\partial p_{f_i}}{\partial \dot{y}_{f_i e}} \ddot{y}_{f_i e} + \dfrac{\partial p_{f_i}}{\partial \psi_{f_i}} \dot{\psi}_{f_i} \end{cases} \tag{39}$$

where β_{1_i} is a nonlinear continuous function, related to the position information of the USV. Because the position information is bounded, β_{1_i} is also bounded. Hypothesis $N_{u_i} > 0$ is the upper bound of β_{1_i}, then $\beta_{1_i} < N_{u_i}$ holds. Similarly, β_{2_i} is bounded, too. Supposing, $N_{p_i} > 0$ is the upper bound of β_{2_i}, then $\beta_{2_i} < N_{p_i}$ holds.

The stability of the control law designed in this paper is proved and the Lyapunov function is constructed as follows:

$$V_{1_i} = \frac{1}{2}s_{1_i}^2 + \frac{1}{2}y_{1_i}^2 + \frac{1}{2}s_{2_i}^2 + \frac{1}{2}y_{2_i}^2 + \frac{1}{2}x_{f_ie}{}^2 + \frac{1}{2}y_{f_ie}{}^2 \quad (40)$$

The derivation and simplification of Eq. (40) is:

$$\begin{aligned}
\dot{V}_{1_i} &= s_{1_i}\dot{s}_{1_i} + y_{1_i}\dot{y}_{1_i} + s_{2_i}\dot{s}_{2_i} + y_{2_i}\dot{y}_{2_i} + x_{f_ie}\dot{x}_{f_ie} + y_{f_ie}\dot{y}_{f_ie} \\
&= s_{1_i}[-\varepsilon_{1_i}\tanh(s_{1_i}) - \eta_{1_i}s_{1_i}] + s_{2_i}[-\varepsilon_{2_i}\tanh(s_{2_i}) - \eta_{2_i}s_{2_i}] \\
&\quad + y_{1_i}(-\frac{y_{1_i}}{T_{1_i}} + \beta_{1_i}) + y_{2_i}(-\frac{y_{2_i}}{T_{2_i}} + \beta_{2_i}) + x_{f_ie}\dot{x}_{f_ie} + y_{f_ie}\dot{y}_{f_ie} \\
&\le -\varepsilon_{1_i}|s_{1_i}| - \eta_{1_i}s_{1_i}^2 - \frac{y_{1_i}^2}{T_{1_i}} + y_{1_i}N_{u_i} - \varepsilon_{2_i}|s_{2_i}| - \eta_{2_i}s_{2_i}^2 - \frac{y_{2_i}^2}{T_{2_i}} + y_{2_i}N_{p_i} \\
&\quad - (k_{1_i}x_{f_ie}{}^2 + k_{2_i}y_{f_ie}{}^2)/w_{f_i} + \sqrt{x_{f_ie}{}^2 + y_{f_ie}{}^2}\sqrt{v_{f_ie}{}^2 + u_{f_ie}{}^2} \qquad (41) \\
&\le -\varepsilon_{1_i}|s_{1_i}| - \eta_{1_i}s_{1_i}^2 - \frac{y_{1_i}^2}{T_{1_i}} + (\alpha_{1_i}y_{1_i}^2 + \frac{N_{u_i}^2}{4\alpha_{1_i}}) - \varepsilon_{2_i}|s_{2_i}| - \eta_{2_i}s_{2_i}^2 - \frac{y_{2_i}^2}{T_{2_i}} + (\alpha_{2_i}y_{2_i}^2 + \frac{N_{p_i}^2}{4\alpha_{2_i}}) \\
&\quad - (k_{1_i}x_{f_ie}{}^2 + k_{2_i}y_{f_ie}{}^2)/w_{f_i} + \sqrt{x_{f_ie}{}^2 + y_{f_ie}{}^2}\sqrt{v_{f_ie}{}^2 + u_{f_ie}{}^2} \\
&\le -\eta_{1_i}s_{1_i}^2 - (\frac{1}{T_{1_i}} - \alpha_{1_i})y_{1_i}^2 + \frac{N_{u_i}^2}{4\alpha_{1_i}} - \eta_{2_i}s_{2_i}^2 - (\frac{1}{T_{2_i}} - \alpha_{2_i})y_{2_i}^2 + \frac{N_{p_i}^2}{4\alpha_{2_i}} \\
&\quad - (k_{1_i}x_{f_ie}{}^2 + k_{2_i}y_{f_ie}{}^2)/w_{f_i} + \sqrt{x_{f_ie}{}^2 + y_{f_ie}{}^2}\sqrt{v_{f_ie}{}^2 + u_{f_ie}{}^2} \\
&\le -\mu_{1_i}V_{1_i} + N_a
\end{aligned}$$

where α_{1_i} and α_{2_i} are positive constants and μ_{1_i} and N_a are:

$$\begin{cases}
\mu_{1_i} = \min(2\eta_{1_i}, \frac{2}{T_{1_i}} - 2\alpha_{1_i}, 2\eta_{2_i}, \frac{2}{T_{2_i}} - 2\alpha_{2_i}, \frac{2k_{1_i}}{w_{f_i}}, \frac{2k_{2_i}}{w_{f_i}}) \\
N_a = \frac{N_{u_i}^2}{4\alpha_{1_i}} + \frac{N_{p_i}^2}{4\alpha_{2_i}} + \sqrt{x_{f_ie}{}^2 + y_{f_ie}{}^2}\sqrt{v_{f_ie}{}^2 + u_{f_ie}{}^2}
\end{cases} \quad (42)$$

Equation (41) is solved as:

$$0 \le V_{1_i}(t) \le N_a/\mu_{1_i} + \left[V_{1_i}(0) - N_a/\mu_{1_i}\right]e^{-\mu_{1_i}t} \quad (43)$$

To facilitate subsequent expressions, the new quantity is defined as follows:

$$\xi = \left[V_{1_i}(0) - N_a/\mu_{1_i}\right]e^{-\mu_{1_i}t} \quad (44)$$

From the above inequality, V_{1_i} is ultimately uniformly bounded. When the time is long enough, ξ tends to zero. Because N_a is bounded, at this point, the convergent limit of V_{1_i} is inclined to zero by choosing appropriate control parameters. The position error, filtering error and sliding surface of formation system x_{f_ie}, y_{f_ie}, y_{1_i}, y_{2_i}, s_{1_i}, s_{2_i} is, ultimately, uniformly bounded and convergent to zero. Therefore, the stability of control law Eq. (24) and (36) is proved and the above control goal of Eq. (7) can be achieved by the designed control law. The formation control of the USVs' formation system is then complete.

SIMULATION VERIFICATION

In order to further prove stability, effectiveness and general applicability of the formation controller designed above, the two cases including circular parallel formation and straight triangle formation are simulated by control law Eq. (24) and (36) in this section; the formation of three USVs are taken as examples. The parameters of the respective USV mathematical models [37] used in the simulation are as follows: $m_{11} = 25.8$, $m_{22} = 33.8$, $m_{33} = 2.76$, $d_{11} = 12 + 2.5|u|$, $d_{22} = 17 + 4.5|v|$, and $d_{33} = 0.5 + 0.1|r|$. The desired trajectory of the leader USV is given in the form of a parametric equation.

CIRCULAR PARALLEL FORMATION

The radius and frequency of the desired circular trajectory of the given leader USV are 20.00 m and 0.05 m, respectively. The mathematical equation is as follows:

$$\begin{cases}
x_d = 20\sin 0.05t \\
y_d = -20\cos 0.05t
\end{cases} \quad (45)$$

According to the actual ocean environment, the values of marine disturbances are chosen as: $\boldsymbol{d}_j = [1 + 4\sin(0.5t), 0.8\sin(0.01t), 1 + 4\sin(0.5t)]^T$.

Table 1 presents the formation information parameters.

Tab. 1. Formation information parameters

Follower USV	L/m	θ/rad
Follower USV 1	5	$\pi/2$
Follower USV 2	5	$-\pi/2$

The initial condition of leader USV, follower USV 1 and follower USV 2 are set as:

$$\begin{cases}
[x_l(0), y_l(0), \psi_l(0), u_l(0), v_l(0), r_l(0)] = [-5\ m, -25\ m, 0\ rad, 0\ m/s, 0\ m/s, 0\ rad/s] \\
[x_{f_1}(0), y_{f_1}(0), \psi_{f_1}(0), u_{f_1}(0), v_{f_1}(0), r_{f_1}(0)] = [-6\ m, -22\ m, 0\ rad, 0\ m/s, 0\ m/s, 0\ rad/s] \\
[x_{f_2}(0), y_{f_2}(0), \psi_{f_2}(0), u_{f_2}(0), v_{f_2}(0), r_{f_2}(0)] = [-6\ m, -32\ m, 0\ rad, 0\ m/s, 0\ m/s, 0\ rad/s]
\end{cases}$$

At the same time, during the simulation experiments, the restrictions on control thrust of the leader USV are: $\tau_{lu\max} = 30N$ and $\tau_{lr\max} = 20N$. The restrictions on control thrust of the follower USV 1 are: $\tau_{f_1u\max} = 30N$ and $\tau_{f_1r\max} = 20N$. Finally, the restrictions on control thrust

of the follower USV 2 are: $\tau_{f_2 u\max} = 30N$ and $\tau_{f_2 r\max} = 15N$ In addition, the changing rate of each USV is also limited, as follows: $d\tau_{lu\max} = 150N/s$, $d\tau_{lr\max} = 100N/s$, $d\tau_{f_1 u\max} = 300N/s$, $d\tau_{f_1 r\max} = 200N/s$, $d\tau_{f_2 u\max} = 150N/s$ and $d\tau_{f_2 r\max} = 100N/s$.

Table 2 presents the controller parameters.

Tab. 2. Controller parameters

	Leader USV	Follower USV 1	Follower USV 2
k_1	4.0	4.1	5.0
k_2	4.0	4.1	5.0
T_1	0.1	0.1	0.1
T_2	0.1	0.1	0.1
λ_1	0.0001	0.0001	0.0001
λ_2	25	30	28
λ_3	0.550	0.055	0.018
η_1	0.10	0.10	0.14
η_2	0.10	0.10	0.14
ε_1	0.010	0.010	0.016
ε_2	0.010	0.010	0.016
C	10	10	10

In order to explain the effect of the designed controller, the circular parallel formation trajectory tracking diagrams, state quantity convergence diagrams, disturbance observer diagrams, and control thrust diagrams are presented. Furthermore, in order to illustrate the role of LVTD for the controller and the whole formation system, circular parallel formation trajectory tracking diagrams without LVTD, control thrust diagrams without LVTD, and comparison diagrams of the position error of the leader USV (with and without LVTD) are shown. The simulation results are given in Figs. 2, 3, 4, 5 and 6.

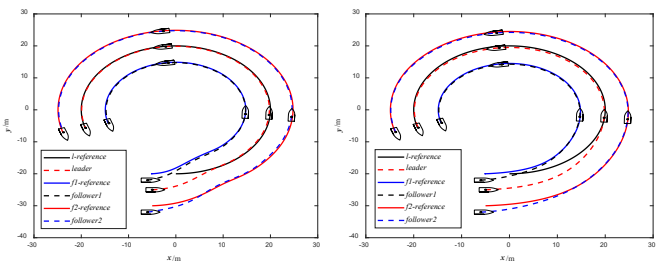

(a) *(b)*

Fig. 2. Formation trajectory tracking results (a) with LVTD (b) without LVTD

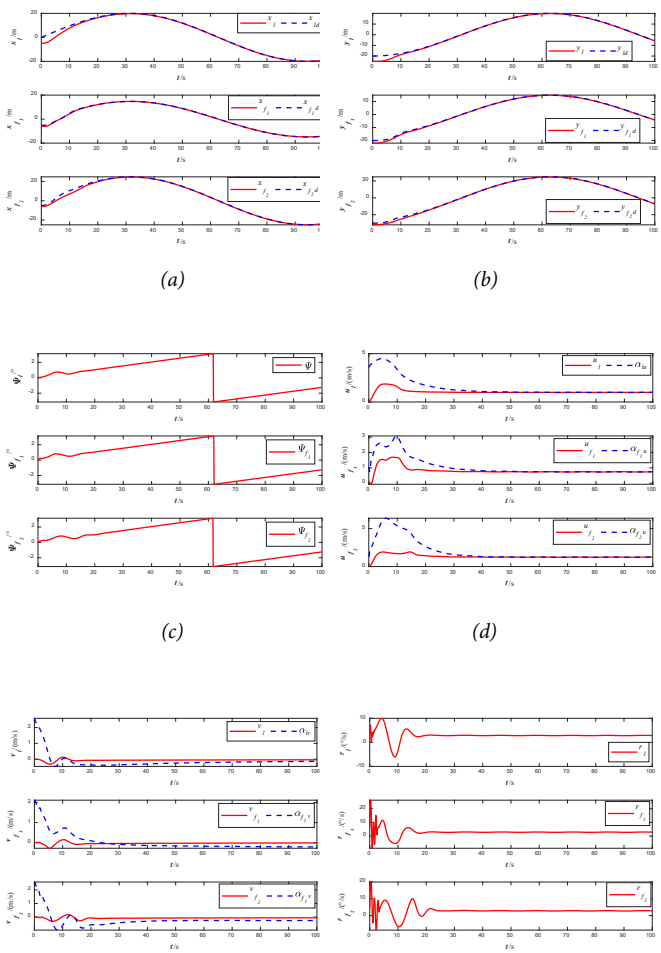

(a) *(b)* *(c)* *(d)* *(e)* *(f)*

Fig. 3. The state quantities of the formation system with LVTD (a) longitudinal position (b) lateral position (c) heading angle (d) longitudinal velocity (e)lateral velocity (f) yawing angular velocity

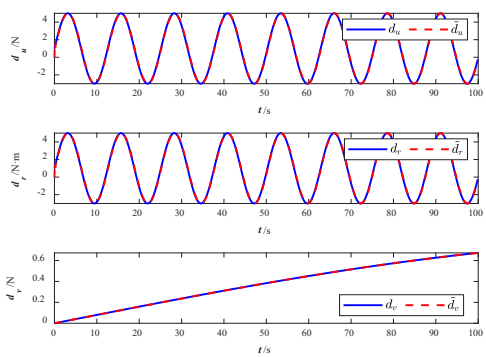

Fig. 4. Disturbances observer

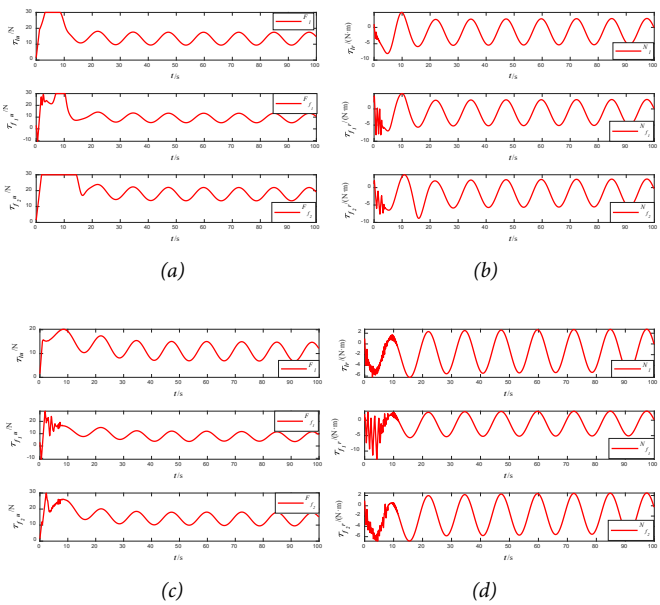

Fig. 5. Control thrust (a) the surge force with LVTD (b) the yaw moment with LVTD (c) the surge force without LVTD (d) the yaw moment without LVTD

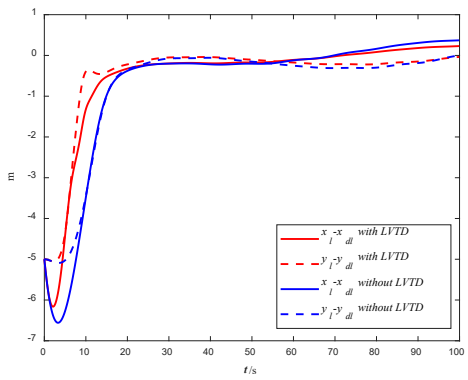

Fig. 6. Position error comparison of leader USV

STRAIGHT TRIANGLE FORMATION

The slope of the desired straight trajectory of the given leader USV is 0.5 and the mathematical formula is as follows:

$$\begin{cases} x_d = 0.5t \\ y_d = 0.25t \end{cases} \tag{46}$$

The values of marine disturbances are chosen to be the same as those above: $\boldsymbol{d}_j = [1+4\sin(0.5t), 0.8\sin(0.01t), 1+4\sin(0.5t)]^T$.

Table 3 gives the formation information parameters.

Tab. 3. Formation information parameters

Follower USV	L/m	θ/rad
Follower USV 1	5	$5\pi/12$
Follower USV 2	5	$-5\pi/12$

The initial conditions of the leader USV, follower USV 1 and follower USV 2 are set as:

$$\begin{cases} [x_l(0), y_l(0), \psi_l(0), u_l(0), v_l(0), r_l(0)] = [0\ m, -4\ m, \pi/2\ rad, 0\ m/s, 0\ m/s, 0\ rad/s] \\ [x_{f_1}(0), y_{f_1}(0), \psi_{f_1}(0), u_{f_1}(0), v_{f_1}(0), r_{f_1}(0)] = [-3m, -9m, \pi/2\ rad, 0\ m/s, 0\ m/s, 0\ rad/s] \\ [x_{f_2}(0), y_{f_2}(0), \psi_{f_2}(0), u_{f_2}(0), v_{f_2}(0), r_{f_2}(0)] = [6m, -8m, \pi/2\ rad, 0\ m/s, 0\ m/s, 0\ rad/s] \end{cases}$$

At the same time, during the simulation experiments, the restrictions on control thrust of the leader USV are: $\tau_{lu\max} = 30N$ and $\tau_{lr\max} = 10N$. The restrictions on control thrust of the follower USV 1 are: $\tau_{f_1u\max} = 40N$ and $\tau_{f_1r\max} = 20N$. Finally, the restrictions on control thrust of the follower USV 2 are: $\tau_{f_2u\max} = 40N$ and $\tau_{f_2r\max} = 15N$. In addition, the changing rate of each USV is also limited: $d\tau_{lu\max} = 350N/s$, $d\tau_{lr\max} = 120N/s$, $d\tau_{f_1u\max} = 350N/s$, $d\tau_{f_1r\max} = 180N/s$, $d\tau_{f_2u\max} = 320N/s$ and $d\tau_{f_2r\max} = 180N/s$.

Table 4 presents the controller parameters.

Tab. 4. Controller parameters

	Leader USV	Follower USV 1	Follower USV 2
k_1	4	6	6
k_2	10	12	12
T_1	0.10000	0.10000	0.00001
T_2	0.10000	0.10000	0.00001
λ_1	0.0001	0.0001	0.0001
λ_2	22	30	15
λ_3	18	20	15
η_1	0.1	0.1	0.1
η_2	0.10	0.02	0.02
ε_1	0.20	0.21	0.22
ε_2	0.20	0.21	0.22
C	10	10	10

Similarly, straight triangle formation trajectory tracking diagrams, state quantity convergence diagrams, disturbances observer diagrams, and control thrust diagrams are presented. The straight triangle formation trajectory tracking diagram without LVTD, control thrust diagram without LVTD, and

the comparison diagram of the position error of the leader USV with and without LVTD are also shown. The simulation results are given in Figs. 7, 8, 9,10 and 11.

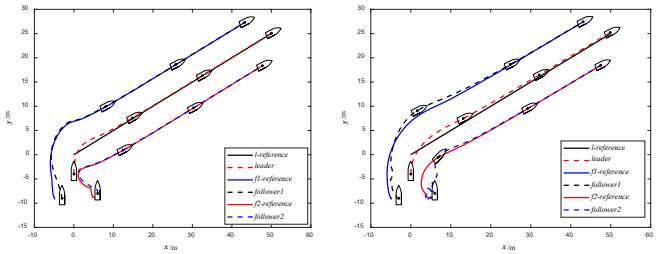

(a) (b)

Fig. 7. Formation trajectory tracking results (a) with LVTD (b) without LVTD

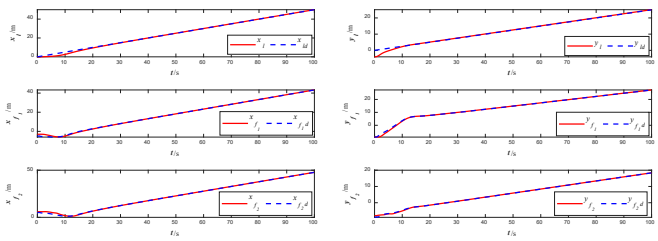

(a) (b)

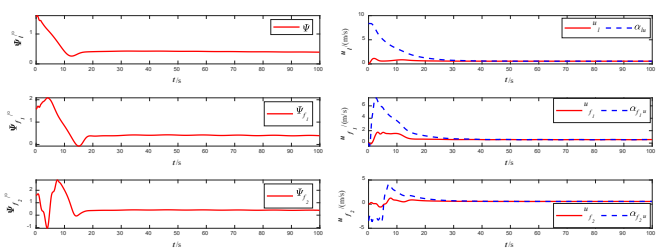

(c) (d)

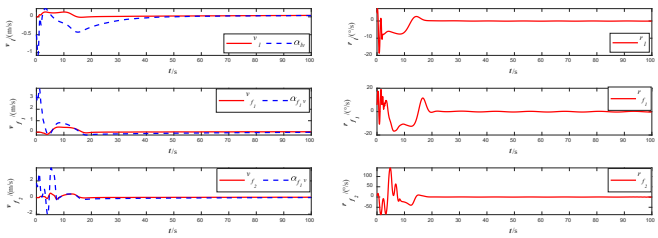

(e) (f)

Fig. 8. The state quantities of formation system with LVTD (a) longitudinal position (b) lateral position (c) heading angle (d) longitudinal velocity (e) lateral velocity (f) yawing angular velocity

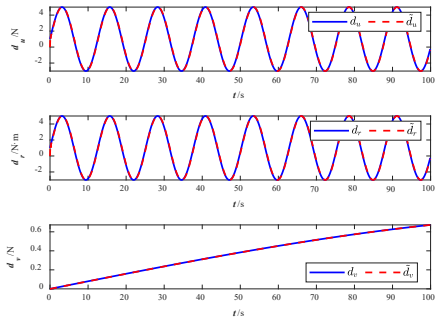

Fig. 9. Disturbances observer

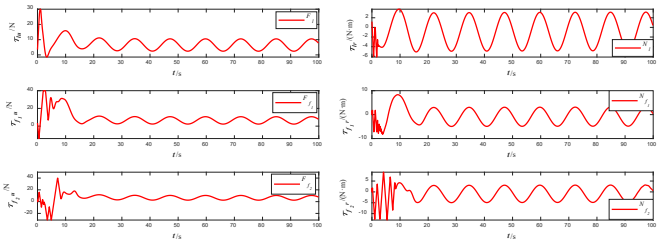

(a) (b)

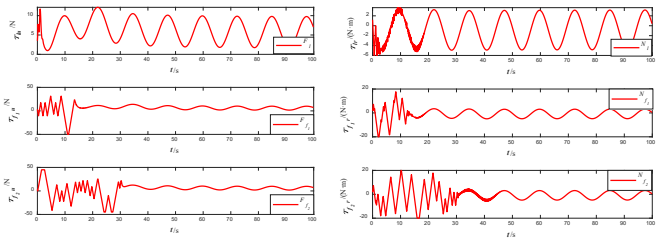

(c) (d)

Fig. 10. Control thrust (a) the surge force with LVTD (b) the yaw moment with LVTD (c) the surge force without LVTD (d) the yaw moment without LVTD

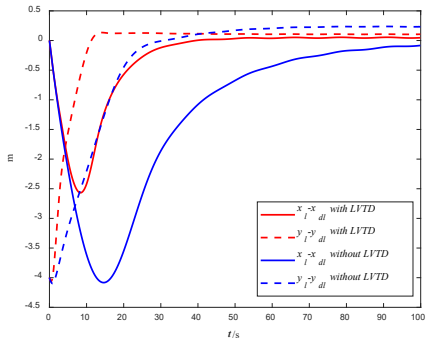

Fig. 11. Position error comparison of leader USV

From the simulation results of the above two cases with LVTD, the convergence time of the formation system is in the range 10~30 seconds; there is no instability or divergence after convergence, which also verifies that the control algorithm proposed in this paper is stable, reliable and effective. The formation trajectory tracking results shown in Fig. 2 and Fig. 7 are without compensation for lateral disturbance but the effect of formation tracking trajectory is still better,

which indicates a certain resistance to disturbance by the controller designed in this paper. In addition, the uncertainty of parameters in the USV mathematical models is considered in the simulation experiments; therefore, the robustness of the designed controller is proved. Figure 3 and Fig. 8 reveal that each state quantity of the USVs changes smoothly and slowly, except yawing angular velocity in Fig. 3(f) and Fig. 8(f). Because the positional error is relatively large during the initial stage of trajectory tracking, the rapidly changing control thrust is input for tracking the desired trajectory by each USV in the formation system as soon as possible; some fluctuation of yawing angular velocity is caused by this. Concurrently, this is also why the surge force and yaw moment in Fig. 5(a)-(b) and Fig. 10(a)-(b) fluctuate. Due to the integral term introduced when stabilising the lateral velocity error, the time taken to stabilise the lateral velocity is longer than other state quantities but the steady-state error is reduced, from Fig. 3(e) and Fig. 8(e). The situation where the nonlinear disturbance observer can observe the variable disturbance is proved in Fig. 4 and Fig. 9.

Through comparison of the simulation results with LVTD and those without LVTD (shown in Fig. 5 and Fig. 10), the oscillation of the controller is reduced due to the introduction of LVTD. Meanwhile, because of the excessive oscillation of the controller without LVTD, the stabilisation time of the formation system is longer and the steady-state error of the formation system is larger, which is indicated in Fig. 6 and Fig. 11. More specifically, from Fig. 6 it can be seen that the stability time of the formation system can be reduced by about 5-10 seconds and the steady-state error of position state quantity can be reduced by about 15 cm, by applying the controller with LVTD. This phenomenon is more obvious in the second case, as Fig. 11 shows that the stability time of the formation system can be reduced by about 50-60 seconds and the steady-state error of the position state quantity can also be reduced by about 15 cm by applying the controller with LVTD. The heading angle of the follower USVs changes greatly in the initial stage of the second case, so the oscillation of the controller without LVTD becomes more intense than the first case, which makes the practical trajectories of the follower USVs shown in Fig. 7(b) not smooth.

CONCLUSION

In this paper, an improved dynamic surface sliding mode control method, combined with tracking, is proposed for the cooperative formation control of underactuated USVs under complex marine environment disturbances. Firstly, based on the backstepping approach idea, the goal of formation control is changed and the virtual control law of longitudinal and lateral velocity is designed for the convenience of subsequent controller design. Then, the first-order low-pass filter about the virtual longitudinal velocity and intermediate state quantity of position is introduced during the stabilisation of the virtual control law of longitudinal and lateral velocity, respectively. Meanwhile, the problem of differential explosion caused by repeated derivation is also solved well. Next, the lateral velocity error with an integral term is considered and introduced for constructing the second-order sliding mode surface, which reduces the steady-state error when stabilising the virtual lateral velocity control law. In addition, the LVTD is designed to smooth the state quantity of lateral velocity in view of the role of TD in ADRC, and the oscillation problem of the controller is successfully avoided. Moreover, combined with the dynamic model of USV, the nonlinear disturbance observer is designed for dealing with complex marine environment disturbances and compensating for them, which makes the design of the controller concise. Finally, the stability and effectiveness of the novel method are verified by Lyapunov stability theory and simulation experiments.

ACKNOWLEDGEMENTS

This work is supported by the Natural Science Foundation of China (Grant numbers 51709214, 51779052, 51809203); Stable Supporting Fund of Science and Technology on Underwater Vehicle Technology (Grant number JCKYS2022SXJQR-04); Innovative Research Foundation of Ship General Performance (Grant number 21822214).

REFERENCES

1. P.N.N. Thanh, P.M. Tom and H.P.H. Anh, 'A new approach for three-dimensional trajectory tracking control of under-actuated AUVs with model uncertainties,' Ocean Engineering, vol. 228, pp. 1-17, May. 2021. doi:10.1016/j.oceaneng.2021.108951.

2. P.J.B. Sanchez, F.P.G. Marquez, S. Govindara, A. But, B. Sportich, S. Marini, V. Jantara and M. Papaelias, 'Use of UIoT for offshore surveys through autonomous vehicles,' Polish Maritime Research, vol. 28, no. 3, pp. 175-189, Oct. 2021. doi:10.2478/pomr-2021-0044.

3. X.Y. Zhou, P. Wu, H.F. Zhang, W.H. Guo and Y.C.Liu, 'Learn to Navigate: Cooperative path planning for unmanned surface vehicles using deep reinforcement learning,' IEEE Access, vol. 7, pp. 165262-165278, Feb. 2019. doi:10.1109/ACCESS.2019.2953326.

4. H.B. Huang, M. Gong, Y.F. Zhuang, S. Sharma and D.G.Xu, 'A new guidance law for trajectory tracking of an underactuated unmanned surface vehicle with parameter perturbations,' Ocean Engineering, vol. 175, pp. 217-222, Mar. 2019. doi:10.1016/j.oceaneng. 2019.02.042.

5. L.G. Li, Z.Y. Pei, J.C. Jin and Y.S. Dai, 'Control of unmanned surface vehicle along the desired trajectory using improved line of sight and estimated sideslip angle,' Polish Maritime Research, vol. 28, no. 2, pp. 18-26, Jul. 2021. doi:10.2478/pomr-2021-0017.

6. S.S. Wang and Y.L. Tuo, 'Robust trajectory tracking control of underactuated surface vehicles with prescribed performance,' Polish Maritime Research, vol. 17, no. 4, pp. 148-156, Dec. 2020. doi:10.2478/pomr-2020-0075.

7. A. Stateczny and P. Burdziakowski, 'Universal autonomous control and management system for multipurpose unmanned surface vessel,' Polish Maritime Research, vol. 26, no. 1, pp. 30-39, Apr. 2019. doi:10.2478/pomr-2019-0004.

8. Z.P. Dong, Y. Liu, H. Wang and T. Qin, 'Method of cooperative formation control for underactuated USVs based on nonlinear backstepping and cascade system theory,' Polish Maritime Research, vol. 28, no. 1, pp. 149-162, Mar. 2021. doi:10.2478/pomr-2021-0014.

9. J.A. Gonzalez-Prieto, C. Perez-Collazo and Y. Singh, 'Adaptive integral sliding mode based course keeping control of unmanned surface vehicle,' Journal of Marine Science and Engineering, vol. 10, no. 1, pp. 1-20, Jan. 2022. doi:10.3390/jmse10010068.

10. J.Y. Zhuang, L. Zhang, Z.H. Qin, H.B. Sun, B. Wang and J. Cao, 'Motion control and collision avoidance algorithm for unmanned surface vehicle swarm in practical maritime environment,' Polish Maritime Research, vol. 26, no. 1, pp.107–116, Apr. 2019. doi:10.2478/ pomr-2019-0012.

11. R.L. Miao, L.X. Wang and S. Pang, 'Coordination of distributed unmanned surface vehicles via model-based reinforcement learning methods,' Applied Ocean Research, vol. 122, pp. 1-15, May. 2022. doi:10.1016/j.apor.2022.103106.

12. L. Rowinski and M. Kaczmarczyk, 'Evaluation of effectiveness of waterjet propulsor for a small underwater vehicle,' Polish Maritime Research, vol. 28, no. 4, pp. 30-41, Jan. 2022. doi: 10.2478/pomr-2021-0047.

13. G.G. Tan, J. Zou, J.Y. Zhuang, L. Wan, H.B. Sun and Z.Y. Sun, 'Fast marching square method based intelligent navigation of the unmanned surface vehicle swarm in restricted waters,' Applied Ocean Research, vol. 95, pp. 1-15, Feb. 2020. doi:10.1016/j.apor.2019.102018.

14. H.N. Esfahani and R. Szlapczynski, 'Model predictive super-twisting sliding mode control for an autonomous surface vehicle,' Polish Maritime Research, vol. 26, no. 3, pp. 163–171, Sept. 2019. doi:10.2478/pomr-2019-0057.

15. X.L. Jiang and G.H. Xia, 'Sliding mode formation control of leaderless unmanned surface vehicles with environmental disturbances,' Ocean Engineering, vol. 244, pp. 1-9, Jan. 2022. doi:10.1016/j.oceaneng. 2021.110301.

16. K. Shojaei, 'Observer-based neural adaptive formation control of autonomous surface vessels with limited torque,' Robotics and Autonomous Systems, vol. 78, pp. 83-96, Apr. 2016. doi: 10.1016/j.robot.2016.01.005.

17. J. Ghommam and M. Saad, 'Adaptive leader-follower formation control of underactuated surface vessels under asymmetric range and bearing constraints,' IEEE Transactions on Vehicular Technology, vol. 67, no. 2, pp. 852-865, Feb. 2018. doi:10.1109/TVT.2017.2760367.

18. D.S. Wang and M.Y. Fu, 'Adaptive formation control for waterjet USV with input and output constraints based on bioinspired neurodynamics,' IEEE Access, vol. 7, pp. 165852-165861, Dec. 2019. doi:10.1109/ACCESS.2019.2953563.

19. S.W. Wang, F. Ma, X.P. Yan, P. Wu and Y.C. Liu, 'Adaptive and extendable control of unmanned surface vehicle formations using distributed deep reinforcement learning,' Applied Ocean Research, vol. 110, pp. 1-28, May. 2021. doi:10.1016/j.apor.2021.102590.

20. L.Y. Chen, H. Hopman and R.R. Negenborn, 'Distributed model predictive control for vessel train formations of cooperative multi-vessel systems,' Transportation Research Part C-Emerging Technologies, vol. 92, pp. 101-118, Jul. 2018. doi:10.1016/j.trc.2018.04.013.

21. M.Y. Fu and L.L. Yu, 'Finite-time extended state observer-based distributed formation control for marine surface vehicles with input saturation and disturbances,' Ocean Engineering, vol. 159, pp. 219-227, Jul. 2018. doi:10.1016/j. oceaneng.2018.04.016.

22. B. Huang, S. Song, C. Zhu, J. Li and B. Zhou, 'Finite-time distributed formation control for multiple unmanned surface vehicles with input saturation,' Ocean Engineering, vol. 233, pp. 1-14, Aug. 2021. doi:10.1016/j. oceaneng.2021.109158.

23. S.L. Dai, S.D. He, H. Lin and C. Wang, 'Platoon formation control with prescribed performance guarantees for USVs,' IEEE Transactions on Industrial Electronics, vol. 65, no. 5, pp. 4237-4246, May. 2018. doi:10.1109/TIE.2017.2758743.

24. J. Ghommam, M. Saad, F. Mnif and Q.M. Zhu, 'Guaranteed performance design for formation tracking and collision avoidance of multiple USVs with disturbances and unmodeled dynamics,' IEEE Systems Journal, vol. 15, no. 3, pp. 4346-4357, Sep. 2021. doi:10.1109/ JSYST.2020.3019169.

25. X. Jin, 'Fault tolerant finite-time leader–follower formation control for autonomous surface vessels with LOS range and angle constraints,' Automatica, vol. 68, pp. 228-236, Jun. 2016. doi:10.1016/j.automatica.2016.01.064.

26. Y. Lu, G.Q. Zhang, Z.J. Sun and W.D. Zhang, 'Robust adaptive formation control of underactuated autonomous surface vessels based on MLP and DOB,' Nonlinear

Dynamics, vol. 94, no. 1, pp. 503-519, Oct. 2018. doi:10.1007/ s11071-018-4374-z.

27. B.S. Park and S.J. Yoo, 'Adaptive-observer-based formation tracking of networked uncertain underactuated surface vessels with connectivity preservation and collision avoidance,' Journal of The Franklin Institute-Engineering and Applied Mathematics, vol. 356, no. 15, pp. 7947-7966, Oct. 2019. doi:10.1016/ j.jfranklin.2019.04.017.

28. H.N. Esfahani, R. Szlapczynski and H. Ghaemi, 'High performance super-twisting sliding mode control for a maritime autonomous surface ship (MASS) using ADP-Based adaptive gains and time delay estimation,' Ocean Engineering, vol. 191, pp. 1-19, Nov. 2019. doi: 10.1016/j. oceaneng.2019.106526.

29. K. Xue and T.Y. Wu, 'Distributed consensus of USVs under heterogeneous UAV-USV multi-agent systems cooperative control scheme,' Journal of Marine Science and Engineering, vol. 9, no. 11, pp. 1-20, Nov. 2021. doi:10.3390/ jmse9111314.

30. S.J. Yoo and B.S. Park, 'Guaranteed-connectivity-based distributed robust event-triggered tracking of multiple underactuated surface vessels with uncertain nonlinear dynamics,' Nonlinear Dynamics, vol. 99, no. 3, pp. 2233-2249, Feb. 2020. doi:10.1007/s11071-019- 05432-5.

31. B.S. Park and S.J. Yoo, 'Connectivity-maintaining and collision-avoiding performance function approach for robust leader–follower formation control of multiple uncertain underactuated surface vessels,' Automatica, vol. 127, pp. 1-10, May. 2021. doi:10.1016/ j.automatica.2021.109501.

32. H.C. Lamraoui and Q.D. Zhu, 'Path following control of fully actuated Autonomous underwater vehicle based on LADRC,' Polish Maritime Research, vol. 25, no. 4, pp. 39-48, Dec. 2018. doi:10.2478/pomr-2018-0130.

33. M. Tomera and K. Podgorski, 'Control of dynamic positioning system with disturbance observer for autonomous marine surface vessels,' Sensors, vol. 21, no. 20, pp. 1-24, Oct. 2021. doi.org/10.3390/s21206723.

34. T. Perez and T.I. Fossen, 'Kinematic models for maneuvering and sea keeping of marine vessels,' Modeling, Identification and Control, vol. 28, no. 1, pp. 19-30, Jan. 2007. doi: 10.4173/ mic.2007.1.3.

35. W.H. Chen, 'Disturbance observer based control for nonlinear systems,' IEEE-ASME Transactions on Mechatronics, vol. 9, no. 4, pp. 706-710, Dec. 2004. doi:10.1109/TMECH. 2004.839034.

36. J.Q. Han, 'From PID to active disturbance rejection control,' IEEE Transactions on Industrial Electronics, vol. 56, no. 3, pp. 900-906, Mar. 2009. doi:10.1109/TIE.2008.2011621.

37. K.D. Do and J. Pan, 'Global robust adaptive path following of underactuated ships,' Automatic, vol. 42, no. 10, pp. 1713-1722, Oct. 2006. doi:10.1016/j.automatica.2006.04.026.

CONTACT WITH THE AUTHORS

Zaopeng Dong

Key Laboratory of High Performance Ship Technology
(Wuhan University of Technology), Ministry of Education,
Wuhan University of Technology, Wuhan;
Science and Technology on Underwater Vehicle Technology
Laboratory, Harbin Engineering University, Harbin, China;
School of Naval Architecture, Ocean and Energy Power
Engineering, Wuhan University of Technology, Wuhan
China

Shijie Qi

Key Laboratory of High Performance Ship Technology
(Wuhan University of Technology), Ministry of Education,
Wuhan University of Technology, Wuhan;
School of Naval Architecture, Ocean and Energy Power
Engineering, Wuhan University of Technology, Wuhan
China

Min Yu
e-mail: yumin@whut.edu.cn

Key Laboratory of High Performance Ship Technology
(Wuhan University of Technology), Ministry of Education,
Wuhan University of Technology, Wuhan;
School of Naval Architecture, Ocean and Energy Power
Engineering, Wuhan University of Technology, Wuhan,
China

Zhengqi Zhang

Key Laboratory of High Performance Ship Technology
(Wuhan University of Technology), Ministry of Education,
Wuhan University of Technology, Wuhan
School of Naval Architecture, Ocean and Energy Power
Engineering, Wuhan University of Technology, Wuhan
China

Haisheng Zhang

Key Laboratory of High Performance Ship Technology
(Wuhan University of Technology), Ministry of Education,
Wuhan University of Technology, Wuhan;
School of Naval Architecture, Ocean and Energy Power
Engineering, Wuhan University of Technology, Wuhan
China

Jiakang Li,

Key Laboratory of High Performance Ship Technology
(Wuhan University of Technology), Ministry of Education,
Wuhan University of Technology, Wuhan;
School of Naval Architecture, Ocean and Energy Power
Engineering, Wuhan University of Technology, Wuhan
China

Yang Liu

Key Laboratory of High Performance Ship Technology
(Wuhan University of Technology), Ministry of Education,
Wuhan University of Technology, Wuhan;
School of Naval Architecture, Ocean and Energy Power
Engineering, Wuhan University of Technology, Wuhan
China